Proceedings of the Thirty-fourth (2024) International Ocean and Polar Engineering Conference **www.isope.org**
Rhodes, Greece, June 16–21, 2024

ISBN 978-1-880653-78-4; ISSN 1098-6189

Hull Form Optimization of KCS Based on Adaptive Sampling Strategy

Yabo Wei, Jianhua Wang, Decheng Wan[*]

Computational Marine Hydrodynamics Lab (CMHL), School of Naval Architecture, Ocean and Civil Engineering,
Shanghai Jiao Tong University, Shanghai, China

[*]Corresponding Author

ABSTRACT

To avoid the time-consuming hydrodynamic performance evaluation of ships via a viscous flow solver in hull form optimization, this paper uses the surrogate model as a data mining tool based on the adaptive sampling method to guide the new sample points to continuously approach the real optimal solution sets in the design space. Firstly, the accuracy and efficiency of the adaptive sampling method are verified by multi-objective mathematical functions. Then, based on this method, the resistance and wake performance of KCS ship at Fr = 0.26 is optimized. In order to reduce the computational workload, a small number of sample points are selected according to the optimal Latin square experimental design method, and then the viscous flow solver naoeFOAM-SJTU is used to evaluate the comprehensive hydrodynamic performance of the deformed ship to establish the surrogate model. The new sample points are searched by the adaptive sampling method, and the surrogate model is updated dynamically until the convergence condition is satisfied to output the optimal solution sets. Compared with the traditional optimization method, the proposed method can greatly reduce the number of required sample points without reducing the optimization accuracy, and further improve the optimization efficiency.

KEY WORDS: hull form optimization; surrogate model; adaptive sampling method; KCS, resistance and wake performance.

INTRODUCTION

With the development of computer technology, the computational fluid dynamics (CFD) method has been widely used. The hydrodynamic performance of ships, such as resistance and seakeeping performance, can be obtained using the CFD method, which provides a numerical tool for comprehensive evaluation of ship hydrodynamic performance for hull form optimization. The simulation-based design (SBD) technology developed on this basis is currently recognized as a hull form optimization method with great advantages (Ni et al., 2020). It integrates the hull deformation method, CFD method, surrogate model, and optimization algorithm, and has received extensive attention in marine fields since it was proposed. Over the past decade, with the development of SBD technology, multi-objective optimization problems have gradually become a research hotspot. Typically, there are two main methods to solve multi-objective optimization problems, of which one is using evolutionary multi-objective algorithms, and the other one is using the weighted sum (WS) method (Sekulski, 2014). Due to the uneven distribution of the optimal solution obtained by the WS method, multi-objective evolutionary algorithms are usually used to solve multi-objective optimization problems (Lin et al., 2018a). The common evolutionary algorithms mainly include the Non-Dominated Sorting Genetic Algorithm-II (NSGA-II) (Miao et al., 2020a; Liu et al., 2021; Liu et al., 2022), the Multi-objective Particle Swarm Optimization Algorithm (MOPSO) (Kim et al.,2016; Su et al., 2019; Tang et al., 2020). In contrast to single-objective problems, there are usually some conflicts between optimization objectives, it is impossible to achieve the best at the same position due to the existence of multiple optimization objectives in multi-objective optimization problems (Lin et al., 2018a). Therefore, when using the evolutionary algorithms mentioned above for optimization, it is usually to optimize at least one objective without deteriorating any one optimization objective. Such optimization is also known as Pareto optimization. Through this multi-objective optimization method, an optimal solution set, also known as the Pareto front (PF), will eventually be obtained. After obtaining this optimization solution set, engineers can select the appropriate optimization solution according to the engineering requirements.

To reduce optimization costs, the surrogate model has been widely employed to replace the expensive CFD evaluation. The surrogate model, also known as the 'black box model', mainly uses a reasonable mathematical model to establish a direct mapping relationship between the design variables and the objective functions in the optimization problems. The commonly used surrogate models include the Kriging model, radial basis function (RBF), artificial neural network (ANN), etc. (Miao and Wan, 2020b; Huang and Chi, 2016; Liu et al., 2020). For example, Lin et al (2018b) applied the Kriging model to optimize the resistance of a twin-skeg ship and obtained the optimal solution whose total resistance was reduced by 5.4 % compared with the original ship. Wang et al (2021) introduced the RBF surrogate model into hull form optimization for the design of the resistance and wake non-uniformity under full load and ballast conditions of a deep-sea aquaculture ship. In addition, the ANN surrogate model was applied to optimize the resistance and seakeeping performance of DTMB5415 (Diez and Serani, 2015).

For the surrogate model-based optimization, it's obvious that the accuracy of the surrogate model is very essential. An inaccurate surrogate model may lead to an invalid optimal solution. To solve this problem, many researchers have proposed different algorithms to improve the accuracy of the surrogate model. Currently, there are mainly two methods: one is to construct a high-quality surrogate model at one time, and the other is to sequentially update the surrogate model with additional sample points. The former requires a reasonable method to sample in the design space. Design of Experiment (DOE) is an effective and widely-used sampling method, it includes orthogonal experimental sampling, Latin hypercube sampling (LHS), optimized Latin hypercube sampling (OLHS), uniform experimental sampling, and so on (Chang et al, 2023). Although those methods mentioned above could be beneficial to improving the accuracy of the surrogate model, there still exist two problems in terms of optimization accuracy and efficiency: 1) lots of samples are needed to guarantee the accuracy of the surrogate model, which will restrict the optimization efficiency; 2) the number of samples depends on personal experience, the optimization design will fail if the samples are not enough and one-time sampling may not guarantee the accuracy of surrogate models of some objectives.

As for the second method, the significant part is to use the information collected in the previous iteration to generate new sampling points, so as to update the surrogate model for the next optimization. Due to its superior error estimation ability, the Kriging model has been widely studied in sequential optimization based on surrogate models. Based on the Kriging model, some sequential sampling methods are studied, which mainly include expected improvement (EI), mean-squared error (MSE), probability of improvement (PI), etc. (Schonlau, 1997; Romero et al., 2015; Jones, 2001). The expected improvement method and its variants have been widely applied to engineering optimization because they can well balance the exploration and exploitation in design space. In this paper, a new optimization system is proposed based on the pseudo expected improvement (PEI) to solve multi-objective optimization problems (Zhan et al., 2017), which is also called sequential sampling-based optimization (SBO) system. The mathematical function is used to test the reliability of this SBO optimization system. Finally, the wake and resistance performance of the KCS ship is optimized using SBD and SBO methods, respectively.

METHODOLOGY

In this section, the principle of the SBO method is introduced, including the surrogate model, adaptive sampling strategy, multi-objective optimization algorithm, termination conditions and the multi-objective optimization system based on the sequential sampling method.

Surrogate model

In this paper, the Kriging model is employed due to its superior error estimation capability.

The Kriging model is a semi-parametric interpolation model composed of two important parts. The first part is a simple regression model with a polynomial change trend, which is used for the global approximation of the model. The second part is the random distribution part representing the surrounding volatility, which is used for the local approximation of the model. These two parts can be expressed by the following formula:

$$\hat{y}_{KRG}(x) = \sum_{i=1}^{l} \beta_{KRGi} f_{KRGi}(x) + \varepsilon_{KRG}(x) \tag{1}$$

where β_{KRGi} is the polynomial regression coefficient, f_{KRGi} denotes the basis function of the polynomial, $\varepsilon_{KRG}(x)$ is the random distribution part of the Kriging model, which satisfies certain statistical characteristics. The mean is 0, the variance is σ^2, and the covariance is not 0, and the covariance expression is as follows:

$$\mathrm{Cov}[\varepsilon_{KRG}(x_i), \varepsilon_{KRG}(x_j)] = \sigma^2 R_{KRG}(x_i, x_j) \tag{2}$$

where $R_{KRG}(x_i, x_j)$ is the correlation function used in the KRG model, which can represent the spatial correlation of sample points. It is mainly related to the distance between points. The functional relationship can be expressed as follows:

$$R_{KRG}(x_i, x_j) = \prod_{p=1}^{N_{KRG}} R_p\left(\theta_p, d_p\right), d_p = \left|x_i^p - x_j^p\right| \tag{3}$$

where N_{KRG} denotes the number of design variables; θ_p is the parameter to be solved.

If the response value corresponding to n sample points $x_1, x_2, \ldots, x_n$ is $y_1, y_2, \ldots, y_n$, the Kriging model is used to predict the response of the predicted point x, and the predicted value is:

$$\hat{y}_{KRG}(x) = f_{KRG}(x)^T \hat{\beta}_{KRG} + r^T(x) {R_{KRG}}^{-1} (y - F_{KRG}\hat{\beta}_{KRG}) \tag{4}$$

In order to obtain the Kriging model with better performance, the parameter $\hat{\beta}_{KRG}$ is obtained by the optimal linear unbiased estimation:

$$\hat{\beta}_{KRG} = \left({F_{KRG}}^T R_{KRG}^{-1} F_{KRG}\right)^{-1} {F_{KRG}}^T {R_{KRG}}^{-1} y \tag{5}$$

The variance σ^2 can be calculated by the following formula:

$$\sigma^2 = \frac{1}{n}(y - F_{KRG}\hat{\beta}_{KRG})^T R_{KRG}^{-1} (y - F_{KRG}\hat{\beta}_{KRG}) \tag{6}$$

It can be seen that the parameter $\hat{\beta}_{KRG}$ and the variance are related to the correlation function, and there is a parameter θ_p to be solved in the correlation function, which can be obtained by solving the following optimization problem by the maximum likelihood estimation method:

$$\max_{\theta_p > 0} \left[-\frac{n}{2}\ln\left(\sigma^2\right) - \frac{1}{2}\ln(|R_{KRG}|) \right] \tag{7}$$

After obtaining the parameter θ_p, the predicted value of the point x can be obtained according to Eq. (4).

Adaptive sampling strategy

In this paper, the pseudo expected improvement (PEI) method which is proposed based on expected improvement (EI) by Zhan et al (2018) is applied to solving multi-objective hull form optimization problems. The EI method is proposed by Jones et al (1998). The expected improvement is expressed in Eq. (8):

$$EI(\mathbf{x}) = \left(y_{\min} - \hat{y}(\mathbf{x})\right)\Phi\left(\frac{y_{\min} - \hat{y}(\mathbf{x})}{s(\mathbf{x})}\right) + s(x)\phi\left(\frac{y_{\min} - \hat{y}(\mathbf{x})}{s(\mathbf{x})}\right) \quad (8)$$

where $y_{\min}$ is the optimal value of the objective function, $\Phi(\mathrm{g})$ and $\phi(\mathrm{g})$ represent the cumulative distribution function and probability density function of the standard normal distribution, respectively, $s(\mathbf{x})$ is the standard deviation of Kriging model.

However, the EI method only selects one sample point, which restricts the efficiency of optimization. Therefore, the PEI method is proposed to select more sample points at once. In multi-objective optimization problems, the $y_{\min}$ is not an optimal value point, but a set of Pareto fronts (PF) which can be expressed as follows:

$$S = \begin{bmatrix} f_1^1 & f_2^1 & \mathrm{L} & f_m^1 \\ f_1^2 & f_2^2 & \mathrm{L} & f_m^2 \\ \mathrm{M} & \mathrm{M} & \mathrm{O} & \mathrm{M} \\ f_1^k & f_2^k & \mathrm{L} & f_m^k \end{bmatrix} \quad (9)$$

where m is the number of objective functions, k is the number of points in PF.

To increase efficiency, the EIM criterion is proposed and it's presented as follows (Zhan et al., 2018):

$$\mathrm{EIM} = \begin{bmatrix} \mathrm{EI}_1^1(\mathbf{x}) & \mathrm{EI}_2^1(\mathbf{x}) & \mathrm{L} & \mathrm{EI}_m^1(\mathbf{x}) \\ \mathrm{EI}_1^2(\mathbf{x}) & \mathrm{EI}_2^2(\mathbf{x}) & \mathrm{L} & \mathrm{EI}_m^2(\mathbf{x}) \\ \mathrm{M} & \mathrm{M} & \mathrm{O} & \mathrm{M} \\ \mathrm{EI}_1^k(\mathbf{x}) & \mathrm{EI}_2^k(\mathbf{x}) & \mathrm{L} & \mathrm{EI}_m^k(\mathbf{x}) \end{bmatrix} \quad (10)$$

To obtain more sample points at once, the PEI method based on the influence function is introduced, and the pseudo expected improvement matrix (PEIM) is provided in Eq. (11), the concrete description can be found in Zhan et al (2018).

$$\begin{bmatrix} \mathrm{PEI}_1^1(\mathbf{x}, q-1) & \mathrm{PEI}_2^1(\mathbf{x}, q-1) & \mathrm{L} & \mathrm{PEI}_m^1(\mathbf{x}, q-1) \\ \mathrm{PEI}_1^2(\mathbf{x}, q-1) & \mathrm{PEI}_2^2(\mathbf{x}, q-1) & \mathrm{L} & \mathrm{PEI}_m^2(\mathbf{x}, q-1) \\ \mathrm{M} & \mathrm{M} & \mathrm{O} & \mathrm{M} \\ \mathrm{PEI}_1^k(\mathbf{x}, q-1) & \mathrm{PEI}_2^k(\mathbf{x}, q-1) & \mathrm{L} & \mathrm{PEI}_m^k(\mathbf{x}, q-1) \end{bmatrix} \quad (11)$$

Each element in the matrix can be expressed as follows:

$$\begin{aligned} \mathrm{PEI}_i^j(\mathbf{x}, q-1) &= \mathrm{EI}_i^j(\mathbf{x}) \times \mathrm{IF}_i(\mathbf{x}, q-1) \\ &= [(f_i^j - \hat{y}_i(\mathbf{x}))\Phi(\frac{f_i^j - \hat{y}_i(\mathbf{x})}{s_i(\mathbf{x})}) + s_i(\mathbf{x})\phi(\frac{f_i^j - \hat{y}_i(\mathbf{x})}{s_i(\mathbf{x})})] \\ &\times \prod_{t=1}^{q-1}\left[1 - \exp(-\sum_{v=1}^{n}\theta_{i,v}|\, x_v - x_v^{(N+t)}|^{p_{i,v}})\right] \end{aligned} \quad (12)$$

where q is the number of sample points that want to be selected at once, IF_i is the influence functions of the i-th surrogate model, n is the number of design variables, $\theta_{i,v}$ and $p_{i,v}$ is the parameters of the i-th surrogate model.

Multi-objective optimization algorithm

To solve multi-objective optimization problems, the Nondominated Sorting Genetic Algorithms (NSGA) are proposed. This algorithm mainly sorts all individuals according to non-dominated sequences and assigns corresponding fitness values according to this ranking. At the same time, in order to ensure the diversity of the population of individuals, a sharing function is added to calculate the distance between different individuals. However, this method still has problems such as complex calculations and a lack of elite strategy. Therefore, Deb, Agrawal and Pratap further improved the problems of this method and formed the NSGA-II algorithm. The basic process of this algorithm is shown in Fig. 1. On the one hand, the elite strategy is introduced to put the excellent individuals contained in the parent generation into the offspring group, so as to avoid the reduction of algorithm efficiency caused by the abandonment of excellent individuals. On the other hand, a crowding comparison operator is introduced to evaluate the population density around the individual, and a more suitable individual is selected by combining crowding and non-dominated sorting. NSGA-II algorithm is a popular, widely used and reliable multi-objective genetic algorithm. This paper uses this algorithm to carry out multi-objective optimization.

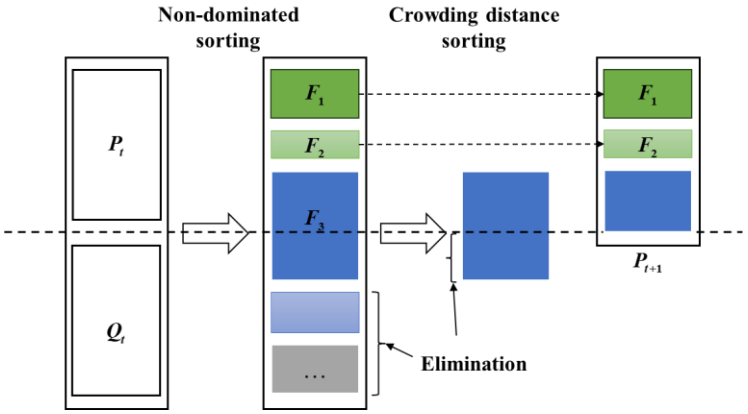

Fig. 1. Flow chart of NSGA-II

Termination conditions

In multi-objective optimization problems, the inverse generation distance (IGD) indicator is usually employed to measure the performance of multi-objective methods on mathematical example. The hypervolume (HV) indicator is usually employed to measure the performance of multi-objective methods on the practical optimization problems because the true Pareto fronts are unknown. According to Wang et al (2021), the definition of IGD and HV are presented as:

1) IGD indicator: Assuming that the true Pareto front of the problem is PF^* and the current Pareto front obtained by the multi-objective optimization algorithm is PF, the IGD is defined as:

$$IGD\left(PF^*, PF\right) = \frac{\sum_{p \in PF^*} d\left(p, PF\right)}{\left|PF^*\right|} \quad (13)$$

where $d\left(p, PF\right)$ is the minimum value of all Euler distances from point p of current PF to point P of the true PF, $\left|PF^*\right|$ is the number of true

PF points. If the IGD value is small, it indicates that the current PF is closer to the real PF .

2) HV indicator: It's the volume of the closed region composed of the current PF and the reference point $\mathrm{r}^* = (r_1^*, r_2^*, \mathrm{L}\ , r_n^*)$, which is defined as:

$$\mathrm{HV}(\mathrm{r}, \mathrm{PF}) = \mathrm{volume}\left(\bigcup_{x \in PF} \left[f_1(x), r_1^* \right] \times \mathrm{L} \times \left[f_n(x), r_n^* \right] \right) \tag{14}$$

where $\mathrm{volume}(\mathrm{g})$ is the Lebesgue measure, $f_n(x)$ is the n-th objective value of a non-dominated solution $\boldsymbol{f} = (f_1, f_2, \mathrm{L}\ , f_\mathrm{m})^\mathrm{T}$ in the solution set PF , $\boldsymbol{r} = (r_1, r_2, \mathrm{L}\ , r_\mathrm{m})^\mathrm{T}$ is the reference points.

In this paper, since the true PFs are known, the termination condition of the SBO optimization system in the process of mathematical functions testing is provided:

$$\left| IGD\left(PF^*, PF_k\right) - IGD\left(PF^*, PF_{k\text{-}1}\right) \right| \le \varepsilon \tag{15}$$

where $IGD\left(PF^*, PF_k\right)$ and $IGD\left(PF^*, PF_{k\text{-}1}\right)$ are the IGD value of approximate PF after the (k-1)-th and k-th iteration, respectively, ε is the threshold value. In this paper, ε=0.001 .

In practical engineering optimization problems, the true PFs are unknown, the termination in Eq. (15) is not unavailable. To solve this problem, the termination condition in practical optimization problems is defined as:

$$\left| \mathrm{HV}(\mathrm{r}, \mathrm{PF}_k) - \mathrm{HV}(\mathrm{r}, \mathrm{PF}_{k-1}) \right| \le \varepsilon \tag{16}$$

where $\mathrm{HV}(\mathrm{r}, \mathrm{PF}_k)$ and $\mathrm{HV}(\mathrm{r}, \mathrm{PF}_{k-1})$ are the HV value of approximate PF after the (k-1)-th and k-th iteration, respectively.

Multi-objective optimization system based on sequential sampling method

Based on the PEI criterion, the SBO-PEI optimization system for multi-objective optimization problems is proposed. Fig. 2 shows the flow chart of the SBO-PEI multi-objective optimization system. The process is described as follows:

1) Suppose that a multi-objective optimization problem has m design variables and n objective functions. m sample points are selected using Optimized Latin Hypercube sampling method.
2) The deformed ships are obtained using deformation methods according to the initial sample set.
3) The hydrodynamic performance of deformed ships is simulated based on our in-house viscous solver naoe-FOAM-SJTU (Ren et al., 2020).
4) The n Kriging model are constructed based on the design variables and hydrodynamic performance of deformed ships.
5) The NSGA-II algorithm is employed to search the approximate PF to evaluate whether the optimization result satisfies the termination condition. If it does, the optimization process will be terminated. Otherwise, proceed with 6).
6) Use the PEI strategy to search n sample points at once and determine whether the new sample point coincides with the existing sample point. The coincidence is eliminated, and the remaining new sample points are retained. Then, proceed with 2) until the termination condition is satisfied.

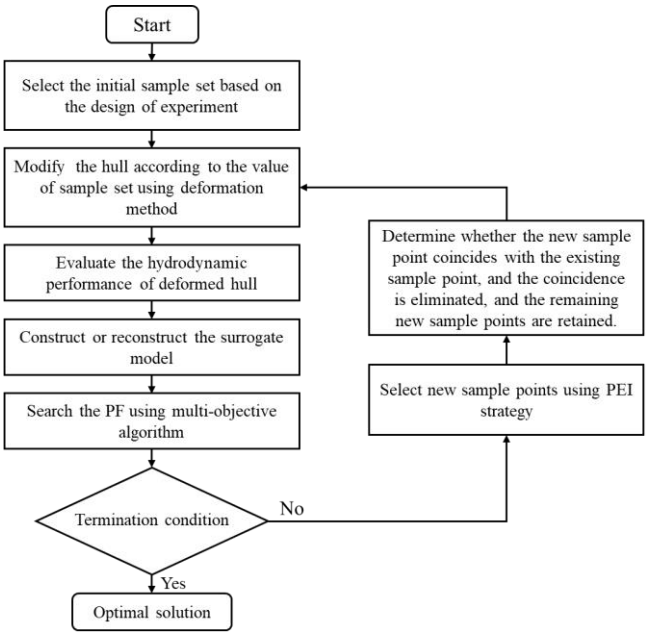

Fig. 2. Flow chart of SBO-PEI multi-objective optimization system

PERFORMANCE TEST USING MATHEMATICAL CASES

To validate the performance of the SBO-PEI optimization system, several common multi-objective optimization problems are adopted for testing. The ZDT1 function and ZDT2 function whose PFs are expressed in Eq. (17) and Eq. (18) (Zitzler et al., 2000). They are tested using SBD optimization system and SBO-PEI optimization system. To obtain meaningful statistical results, each optimization system is run 20 times on each optimization problem. The test results are shown in Table 1.
It can be seen that the ZDT1 and ZDT2 functions only need an average of 44.2 and 58.3 sample points to satisfy the convergence condition, respectively.

$$\begin{cases} \min\ f_1(\mathbf{x}) = x_1, \\ \min\ f_2(\mathbf{x}) = g(\mathbf{x})\left[1 - \sqrt{f_1(\mathbf{x}) / g(\mathbf{x})}\right], \\ g(\mathbf{x}) = 1 + 9 \sum_{i=2}^{m} x_i / (m-1) \\ \mathrm{s.t.} 0 < x_i < 1, \boldsymbol{i} = 1, 2, 3 \end{cases} \tag{17}$$

$$\begin{cases} \min\ f_1(\mathbf{x}) = x_1, \\ \min\ f_2(\mathbf{x}) = g(\mathbf{x})\left[1 - (f_1(\mathbf{x}) / g(\mathbf{x}))^2\right], \\ g(\mathbf{x}) = 1 + 9 \sum_{i=2}^{m} x_i / (m-1) \\ \mathrm{s.t.} 0 < x_i < 1, \boldsymbol{i} = 1, 2, \mathrm{K}\ , 6 \end{cases} \tag{18}$$

Table 1. Test results

Test functions	Num of design variables	Num of sample points based on SBO-PEI
ZDT1	3	54.20
ZDT2	6	59.25

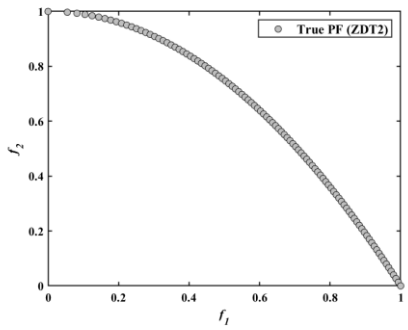

Fig. 3. True PF of ZDT2

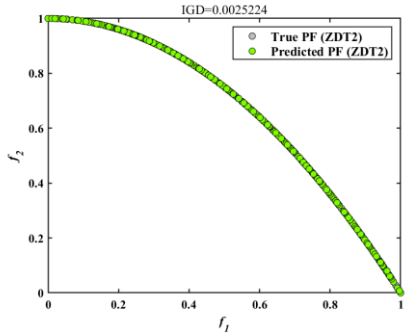

Fig. 4. Predicted PF using NSGA-II algorithm

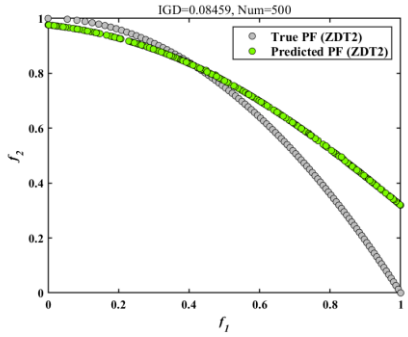

Fig. 5. Predicted PF using SBD optimization system

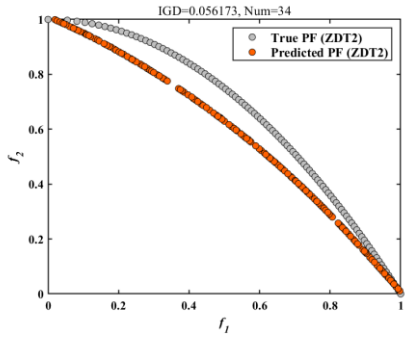

(a) N=34

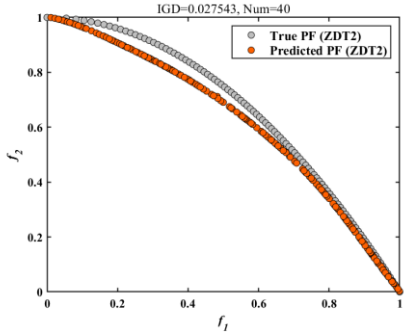

(b) N=40

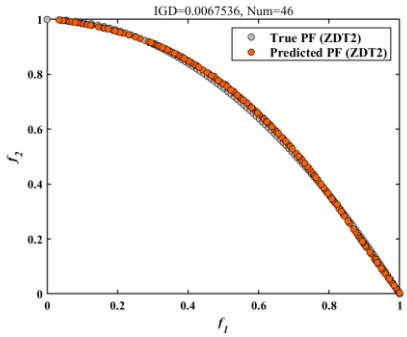

(c) N=46

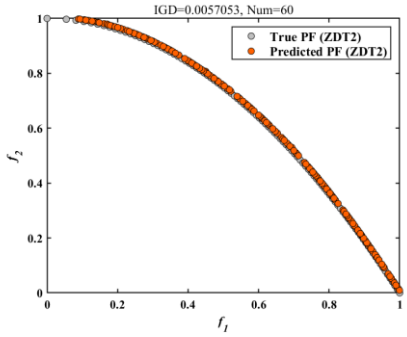

(d) N=60

Fig. 6. Iteration process of ZDT2 using SBO-PEI optimization system

Fig.3 and Fig.4 show the true PF of the ZDT2 function and predicted PF using NSGA-II algorithm. Besides, Fig.5 shows the predicted PF using 500 sample points based on the SBD optimization system, it can be seen that there is a significant difference between the predicted PF and the real PF. One of the iteration processes based on SBO-PEI optimization system is shown in Figure 6, only 56 are needed to obtain the optimal solutions.

HULL FORM OPTIMIZATION OF KCS

Model and definition of optimization problems

The model and principal dimensions of KCS are shown in Fig. 7 and Table 2.

Fig. 7. Model of KCS

Table 2. Principal dimensions of KCS

	Unit	Full scale	Model scale
L_{pp}	m	230	7.2786
L_{wl}	m	232.5	7.3576
B_{wl}	m	32.2	1.019
T	m	10.8	0.342

The wake performance and resistance performance of KCS at Fr=0.26 are optimized using SBD optimization system and SBO-PEI optimization system, respectively. The objective functions are defined as:

$$f_1 = \frac{R_t}{R_t^{org}} \tag{19}$$

$$f_2 = 1 - w_n \tag{20}$$

where R_t is the total resistance of the deformed ships, R_t^{org} is the total resistance of the mother ship, w_n is the nominal wake coefficient.

Numerical calculations

Based on our in-house viscous naoe-FOAM-SJTU, the resistance and wake performance of KCS are calculated. Three sets of different density grids (fine grid, medium grid and rough grid) are divided, and the convergence of the resistance and wake performance is verified. The three sets of grids adopt the same encryption method, and the background grid of the adjacent sets of grids is $\sqrt{2}$ times in the direction of each coordinate axis. The number of three sets of grids is shown in Table 3. The three sets of computational grids are shown in Figure 8.

Table 3. Number of three sets of grids

	Background grid number	Total grid number
S3	85×14×42	1252687
S2	120×20×60	3586346
S1	170×28×84	8448150

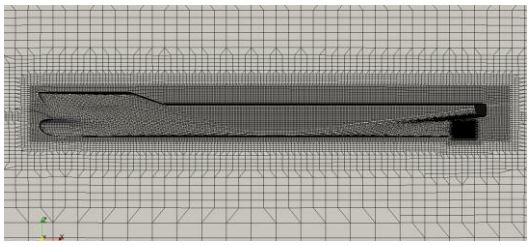

(a) Coarse (S3)

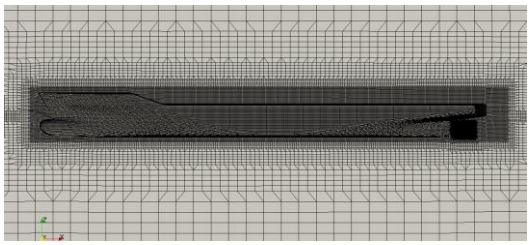

(b) Medium (S2)

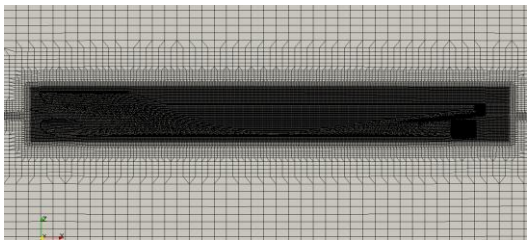

(c) Fine (S1)

Fig. 8. Three sets of meshes

The error between the mesh size of the three sets of grids and the calculated resistance coefficient and wake performance compared with the experimental results (Hino, 2005) are shown in Table 4. In order to save computing resources, the medium grid will be used for subsequent optimization.

Table 4. Number of three sets of grids

	Rt(CFD)	Ct(CFD)	Ct(EFD)	1-w_n (CFD)	1-w_n (EFD)
S3	39.42	0.00343	0.00355	0.651	0.686
S2	40.60	0.00353	0.00355	0.667	0.686
S1	40.93	0.00356	000355	0.674	0.686

Geometric reconstruction

In this paper, the free form deformation (FFD) method (Liu et al., 2023) and the shifting method are used to modify the hull lines of KCS. The deformation parameters are shown in Table 5 and the deformation diagrams are shown in Fig. 9 and Fig. 10.

Table 5. Deformation parameters

Parameters	Range
α_{1f}	[-0.036,0.036]
α_{2f}	[0.3,0.4]
x_1	[-0.035,0.025]
y_1	[-0.015,0.015]
z_1	[-0.018,0.018]
x_2	[-0.035,0.035]
y_2	[-0.05,0.05]
y_3	[-0.065,0.065]

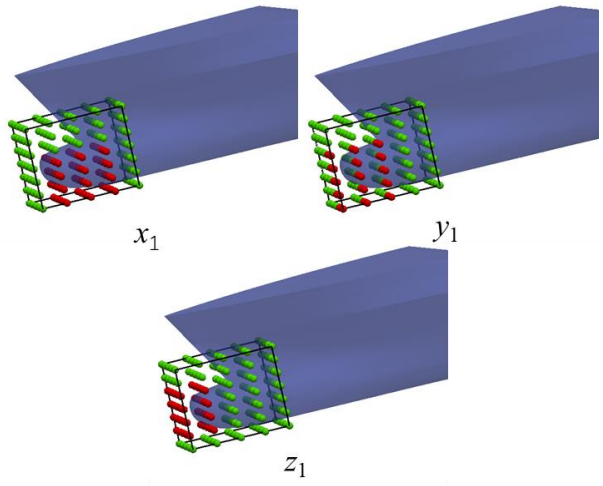

(a) Bow deformation diagrams

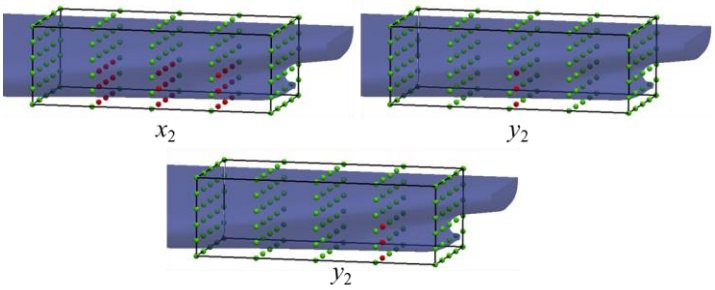

(b) Stern deformation diagrams

Fig. 9. Deformation diagrams of KCS using FFD method

Fig. 10. Deformation diagrams of KCS using shifting method

Optimization results

The wake and resistance performance of KCS is optimized by using the SBD optimization system and SBO-PEI optimization system, respectively. 80 sample points are selected using OLHS at once in the SBD optimization system and 8 sample points are selected in the SBO-PEI optimization system. The extra sample points will be selected according to the flow chart of Fig. 2. The iteration of HV is shown in Fig.11 and the convergence is achieved. Fig.12 shows the PF obtained using SBD optimization system and SBO-PEI optimization system.

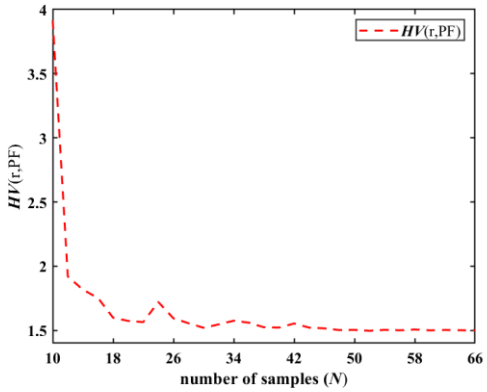

Fig. 11. Convergence curve of HV value

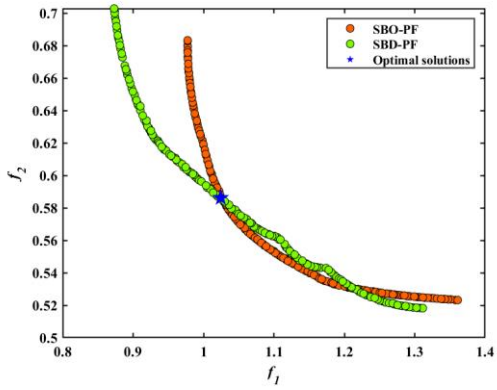

Fig. 12. Pareto fronts of two optimization systems

As shown in Fig.12, the optimal solutions are extracted from the overlap of PF obtained by the two optimization systems. The specific parameters are shown in Table 6. The simulation results are shown in Table 7. It can be seen from Fig.12 and Table 7 that the optimization prediction results obtained by the SBO-PEI optimization system are closer to the numerical results, reflecting that the SBO-PEI optimization system has higher prediction accuracy near the Pareto optimal solution set of the multi-objective optimization problem.

Table 6. Optimal solutions

Parameters	SBD	SBO
α_{1f}	0.0144	0.0163
α_{2f}	0.3995	0.3916
x_1	-0.0122	-0.0096
y_1	0.0099	0.0148
z_1	-0.0164	0.0104
x_2	0.0348	0.035
y_2	-0.0109	0.045
y_3	-0.0638	-0.0576

Table 7. Comparison of the resistance and wake of initial and optimal hulls

	Kriging (f_1)	CFD (f_1)	Δf_1	Kriging (f_2)	CFD (f_2)	Δf_2
initial	-	1.0	-	-	0.667	-
SBD	1.0259	1.0872	8.72%	0.5851	0.5730	-14.09%
SBO	1.0260	1.0201	2.01%	0.5852	0.5853	-12.25%

CONCLUSIONS

As the optimization problems become more complicated, it's tough to build a surrogate with great accuracy at once. To a large extent, it depends on the quantity and quality of sample points. Therefore, the traditional SBD technology is difficult to be adopted. The dynamic approximation model technology based on some filling criteria is born.

In this paper, a new optimization system based on PEI criteria is proposed for hull form optimization. To verify the reliability of this method, the multi-objective mathematical functions are tested first, and then the resistance and wake performance of KCS are optimized based on SBD optimization system and SBO-PEI optimization system. Through testing, it is found that the SBO-PEI method can use fewer sample points to obtain better results. In the optimization example, the SBO-PEI method only needs 66 sets of sample points, and the optimization efficiency is improved by 17.50 %.

This paper only studies the EI and its variants and does not pay attention to other filling criteria. In the future, other fill criteria will be studied and applied to more complex optimization problems to further prove their accuracy and efficiency. Besides, how many sample points to add in each iteration is needed to be further discussed.

ACKNOWLEDGMENTS

This work is supported by the National Natural Science Foundation of China (52131102), to which the authors are most grateful.

REFERENCES

Chang H, Liu Z, Zhan C, et al. Sampling method for hull form optimization based on the morphing method and its application[J]. *Ocean Engineering*, 2023, 281: 114715.

Deb K, Agrawal S, Pratap A, et al. A fast elitist non-dominated sorting genetic algorithm for multi-objective optimization: NSGA-II[C]//*Parallel Problem Solving from Nature PPSN VI: 6th International Conference Paris, France, September 18–20, 2000 Proceedings 6*. Springer Berlin Heidelberg, 2000: 849-858.

Diez M, Serani A, Campana E F, et al. Multi-objective hydrodynamic optimization of the DTMB 5415 for resistance and seakeeping[C]//*SNAME International Conference on Fast Sea Transportation*. SNAME, 2015: D021S005R012.

Hino T. Proceedings of CFD workshop Tokyo 2005[J]. Tokyo, Japan, 2005.

Huang F, Chi Y. Hull form optimization of a cargo ship for reduced drag[J]. *Journal of Hydrodynamics*, Ser. B, 2016, 28(2): 173-183.

Jones D R. A taxonomy of global optimization methods based on response surfaces[J]. *Journal of global optimization*, 2001, 21: 345-383.

Jones D R, Schonlau M, Welch W J. Efficient global optimization of expensive black-box functions[J]. *Journal of Global optimization*, 1998, 13: 455-492.

Kim H J, Choi J E, Chun H H. Hull-form optimization using parametric modification functions and particle swarm optimization[J]. *Journal of marine science and technology*, 2016, 21: 129-144.

Lin C, Gao F, Bai Y. An intelligent sampling approach for metamodel-based multi-objective optimization with guidance of the adaptive weighted-sum method[J]. *Structural and Multidisciplinary Optimization*, 2018a, 57: 1047-1060.

Lin Y, He J, Li K. Hull form design optimization of twin-skeg fishing vessel for minimum resistance based on surrogate model[J]. *Advances in Engineering Software*, 2018b, 123: 38-50.

Liu Z, Liu X, Wan D. Wigley Hull Design Optimization Based on Artificial Neural Network and Genetic Algorithm[C]//*ISOPE Pacific/Asia Offshore Mechanics Symposium. ISOPE*, 2020: ISOPE-P-20-196.

Liu X, Wan D, Lei L. Multi-fidelity model and reduced-order method for comprehensive hydrodynamic performance optimization and prediction of JBC ship[J]. *Ocean Engineering*, 2023, 267: 113321.

Liu X, Zhao W, Wan D. Hull form optimization based on calm-water wave drag with or without generating bulbous bow[J]. *Applied Ocean Research*, 2021, 116: 102861.

Liu Z, Zhao W, Wan D. Resistance and wake distortion optimization of JBC considering ship-propeller interaction[J]. *Ocean Engineering*, 2022, 244: 110376.

Miao A, Wan D. Hull form optimization based on an NM+ CFD integrated method for KCS[J]. *International Journal of Computational Methods*, 2020a, 17(10): 2050008.

Miao A, Zhao M, Wan D. CFD-based multi-objective optimisation of S60 Catamaran considering Demihull shape and separation[J]. *Applied Ocean Research*, 2020b, 97: 102071.

Ni Q, Ruan W, Li S, et al. Multiple speed integrated optimization design for a SWATH using SBD technique[J]. *Journal of Marine Science and Technology*, 2020, 25: 185-195.

Ren Z, Wang J, Wan D. Investigation of the flow field of a ship in planar motion mechanism tests by the vortex identification method[J]. *Journal of Marine Science and Engineering*, 2020, 8(9): 649.

Romero D A, Marin V E, Amon C H. Error metrics and the sequential refinement of kriging metamodels[J]. *Journal of Mechanical Design*, 2015, 137(1): 011402.

Schonlau M. Computer experiments and global optimization[J]. 1997.

Sekulski Z. Ship hull structural multi-objective optimization by evolutionary algorithm[J]. *Journal of Ship Research*, 2014, 58(02): 45-69.

Su S, Han J, Xiong Y. Optimization of unmanned ship's parametric subdivision based on improved multi-objective PSO[J]. *Ocean Engineering*, 2019, 194: 106617.

Tang Q, Li Y, Deng Z, et al. Optimal shape design of an autonomous underwater vehicle based on multi-objective particle swarm optimization[J]. *Natural Computing*, 2020, 19: 733-742.

Wang P, Chen Z, Feng Y. Many-objective optimization for a deep-sea aquaculture vessel based on an improved RBF neural network surrogate model[J]. *Journal of Marine Science and Technology*, 2021, 26: 582-605.

Wang Z, Zhang Q, Ong Y S, et al. Choose appropriate subproblems for collaborative modeling in expensive multi-objective optimization[J]. *IEEE Transactions on Cybernetics*, 2021, 53(1): 483-496.

Zhan D, Qian J, Liu J, et al. Pseudo expected improvement matrix criteria for parallel expensive multi-objective optimization[C]//Advances in Structural and Multidisciplinary Optimization: Proceedings of the 12th World Congress of Structural and Multidisciplinary Optimization (WCSMO12) 12. *Springer International Publishing*, 2018: 175-190.

Zitzler, Eckart, Kalyanmoy Deb, and Lothar Thiele. "Comparison of multi-objective evolutionary algorithms: Empirical results." *Evolutionary computation* 8.2 (2000): 173-195.